

Analytical Methods

Accepted Manuscript



This is an *Accepted Manuscript*, which has been through the Royal Society of Chemistry peer review process and has been accepted for publication.

Accepted Manuscripts are published online shortly after acceptance, before technical editing, formatting and proof reading. Using this free service, authors can make their results available to the community, in citable form, before we publish the edited article. We will replace this *Accepted Manuscript* with the edited and formatted *Advance Article* as soon as it is available.

You can find more information about *Accepted Manuscripts* in the [Information for Authors](#).

Please note that technical editing may introduce minor changes to the text and/or graphics, which may alter content. The journal's standard [Terms & Conditions](#) and the [Ethical guidelines](#) still apply. In no event shall the Royal Society of Chemistry be held responsible for any errors or omissions in this *Accepted Manuscript* or any consequences arising from the use of any information it contains.

**A sensitive colorimetric aptasensor for chloramphenicol detection in fish and
pork based on the amplification of nano peroxidase-polymer**

Huiju Gao^a, Ning Gan^{b*}, Daodong Pan^{a, c*}, Yinji Chen^d, Tianhua Li^b, Yuting Cao^b,
Tian Fu^a

^a Key Laboratory of Animal Protein Food Deep Processing Technology of Zhejiang,
Ningbo University, Ningbo 315211, P. R. China

^b State Key Laboratory Base of Novel Functional Materials and Preparation Science,
Faculty of Materials Science and Chemical Engineering, Ningbo University, Ningbo
315211, P. R. China.

^c Food Science & Nutrition Department, Nanjing Normal University, Nanjing 210097,
P. R. China

^d College of Food Science & Engineering, Nanjing University of Financial and
Economics, Nanjing 210007, P. R. China

*Corresponding author:

Ning Gan, Daodong Pan

E-mail: ganning@nbu.edu.cn

E-mail: daodongpan@163.com

Tel: +86-574-87609987; Fax: +86-574-87609987.

Tel: +86-574-87608347; Fax: +86-574-87608347.

Abstract

1
2
3
4
5
6
7
8
9
10
11
12
13
14
15
16
17
18
19
20
21
22
23
24
25
26
27
28
29
30
31
32
33
34
35
36
37
38
39
40
41
42
43
44
45
46
47
48
49
50
51
52
53
54
55
56
57
58
59
60

A novel colorimetric aptasensor was developed for sensitive and selective determination of chloramphenicol (CAP) based on gold nanoparticles (AuNPs) labeled with Power Vision (PV) and magnetic separation. The PV, with a high enzyme-to-antibody ratio, is composed of a compact enzyme-linker antibody conjunction. In this assay, the aptamer of CAP was immobilized on Fe₃O₄@Au magnetic nanoparticles as capture probe (AuMNPs-Apt) to concentrate target CAP. The complementary DNA (cDNA) and PV were both labeled on AuNPs to form a nano-peroxidase polymer as signal tag (cDNA-AuNPs-PV). And the special tags could hybridize with aptamer and cDNA to form AuMNPs-Apt/cDNA-AuNPs-PV conjugates. In the presence of CAP, the aptamer preferentially bound with CAP and caused the dissociation of some cDNA-AuNPs-PV on the conjugates with magnetic separation. PV, carried on signal tags, could greatly catalyze 3,3',5,5'-tetramethylbenzidine (TMB) for color development, which could be quantified by Ultraviolet-visible (UV-vis) spectroscopy. Linear response to CAP concentration in the range of 0.05-200 ng mL⁻¹ was measured with this proposed method, with low detection limit down to 0.02 ng mL⁻¹. Besides, this assay was successfully employed to analyze CAP in fish and pork samples, whose results were consistent with conventional enzyme-linked immunosorbent assay (ELISA) method.

1 Introduction

Chloramphenicol (CAP) is an effective broad spectrum antibiotic, which can inhibit the activity of both Gram-positive and Gram-negative bacteria.^{1,2} Recent researches have demonstrated that CAP is a suspected carcinogen which may cause deathful side effects such as aplastic anemia and hypersensitivity in humans, and even low concentration of CAP may lead to seriously adverse influence.^{3,4} Therefore, some countries, such as USA, Canada and China, have banned the use of CAP in food-producing animals. However, CAP is still illegally used in some major food-producing animals all over the world due to its highly effective, accessibility, low cost.^{5,6} CAP residues have been found in different food samples, such as crop, honey, shrimp, poultry meat, and milk.⁷⁻¹⁰ Considering the efficiency, developing a specific and sensitive method for the detection of CAP residues in food samples is therefore of great significance.

To date, the commonly existing methods and strategies to determine CAP are as follows: high-performance liquid chromatography (HPLC),^{11,12} liquid chromatography-tandem mass spectrometry,¹³ enzyme linked immunosorbent assay (ELISA)¹⁴ and electrochemical sensors,^{15,16} etc. Some of these methods above have been successfully applied in real samples determination. However, there are still some limitations in practical applications for these assays. Some of them are time-consuming for sample preparation, some require a great amount of organic solvents and some need valuable apparatus. Although ELISA method is quick, simple and visible, there still exists some challenges. And the LOD of commercial ELISA

1
2
3
4 method to detect CAP was 0.11 ng mL^{-1} according to the kit's protocol (Product ID:
5
6 HE09001). The ELISA Kit's price is very high, which due to that the antibodies being
7
8 employed to detect small moleculars are usually expensive. Moreover, the
9
10 immunizing potency of the same antibody in different batch is very different owing to
11
12 their preparation from different animal sources and thus heavily limits their wide
13
14 application. Therefore, a new bio-receptor based biosensor for analytical application is
15
16 an urgent need.
17
18
19

20
21 Aptamers (ssDNA) are single-stranded DNA or RNA sequences that could be in
22
23 vitro synthesized with systematic evolution of ligands by the exponential enrichment
24
25 (SELEX).¹⁷ Aptamers are cost-effective, reproducible, animal-friendly, stable and can
26
27 be produced faster than antibodies. And aptamers are nucleic acid ligands that are able
28
29 to specifically and selectively recognize a given target alternatives to antibodies.¹⁸
30
31 Thus, aptamers have been extensively used as promising alternative bio-receptors in a
32
33 widespread variety of analytical applications.¹⁹⁻²¹ Moreover, colorimetric assays are
34
35 becoming well known techniques and commonly used for routine analysis due to its
36
37 low cost and simplicity.²² Hence, aptamer-based colorimetric biosensors have gained
38
39 considerable concern and become one of the predominant analytical techniques with
40
41 the advantages of high chemical stability, low cost, feasibility, and ease of
42
43 observation.²³⁻²⁵ Luo et al. developed a simple colorimetric sensing method to detect
44
45 *invA* gene of *Salmonella* by using DNzyme probe self-assembled AuNPs as signal
46
47 tags.²³ Liu et al. have designed a colorimetric aptasensor for the determination of
48
49 8-hydroxy-2'-deoxyguanosine based on G-quadruplex-hemin DNzyme.²⁶ However,
50
51
52
53
54
55
56
57
58
59
60

1
2
3 the obtained absorbance signals are usually restricted by the detection tracers' density.
4
5
6 Therefore, rapid and sensitive strategies are required to achieve an amplification
7
8
9 signal.

10
11 Nowadays, one of the most widely used tracers in aptasensor is horseradish
12
13 peroxidase (HRP), which can catalyze a variety of substrates, such as
14
15 3,3'-diaminobenzidine tetrahydrochloride (DAB), 3,3',5,5'-tetramethylbenzidine
16
17 (TMB), to form colored products. During this measurement, the color change is
18
19 mainly due to the catalytic reaction of enzymes toward substrates.²⁷ Hence, the
20
21 detection sensitivity is always hindered by the amount of enzymes to some extent. To
22
23 solve this problem, our goal in this study is to exploit a novel tracer for developing a
24
25 colorimetric aptasensor with high sensitivity. Therefore, a more compact
26
27 enzyme-linker antibody conjugate, such as PowerVision (PV) is urgently needed. The
28
29 PV is derived from a compact enzyme-linker linear polymer, which was composed of
30
31 a great number of enzyme molecules (about more than 100 HRPs in one polymer
32
33 chain).²⁸ To achieve the high sensitivity, gold nanoparticles (AuNPs) have been the
34
35 most widely used in different biosensing assays for signal amplification because of its
36
37 high surface-to-volume ratio and good biocompatibility.²⁹⁻³¹ Hence, in this study, PV
38
39 is incubated with the AuNPs, the resulting copolymers (AuNPs-PV) act as highly
40
41 sensitive signal tags, which could greatly catalyze the oxidation of TMB for color
42
43 development and produce superior detection efficiency. Moreover, the capture probes'
44
45 preparation steps were friendly and inexpensive. It was prepared only by Au-S bond
46
47 self-assembling and DNA hybrid technique without other chemical derivatization.
48
49
50
51
52
53
54
55
56
57
58
59
60

1
2
3
4
5
6
7
8
9
10
11
12
13
14
15
16
17
18
19
20
21
22
23
24
25
26
27
28
29
30
31
32
33
34
35
36
37
38
39
40
41
42
43
44
45
46
47
48
49
50
51
52
53
54
55
56
57
58
59
60

Herein, we fabricated a novel colorimetric aptasensor for detecting CAP based on PV functionalized AuNPs for signal amplification with magnetic separation. Scheme 1 illustrated the developed strategy. Specifically, aptamer coated $\text{Fe}_3\text{O}_4@Au$ magnetic nanoparticles ($\text{Fe}_3\text{O}_4@Au\text{-Apt}$) is utilized to capture and concentrate target CAP with high affinity and specificity. It also allows for easy removal of excess CAP under high magnetic field, which facilitates efficient extraction. In the next step, PV, which was connected to complementary DNA/AuNPs and used as signal tags (cDNA-AuNPs-PV). Subsequently, this designed signal tags hybridized with aptamer and cDNA to form AuMNP-Apt/cDNA-AuNPs-PV conjugates. Upon adding CAP, some signal tags could be dissociated into the supernatant due to the higher affinity between CAP and aptamer. The PV on signal tags could catalyze the oxidation of TMB, generating a colorimetric signal, which can be monitored simply by naked eye or detected by Ultraviolet-visible (UV-vis) spectroscopy. This technique provides a promising alternative way for real-time monitoring of CAP residues in food with a sensitive and selective strategy.

Scheme.1

2 Experimental

2.1 Materials

The oligonucleotides used in this experiment were purchased from Shanghai Sangon Biological Engineering Technology & Services Co., Ltd. (Shanghai, China). With the following sequences: thiolated aptamer, 5'SH-(CH₂)₆-ACT TCA GTG AGT TGT CCC ACG GTC GGC GAG TCG GTG GTA G-3' was chosen according to the

1
2
3
4 previously reported literature;^{32,33} thiolated complementary DNA, 5'SH-(CH₂)₆-TTT
5
6 TCT ACC ACC GAC TCG C-3'. CAP ELISA kit was supplied by Huaan Magnech
7
8 Bio-tech Co., Ltd. (Beijing, China) and PowerVision was purchased from GBI Co.,
9
10 Ltd. (Mukilteo, WA, USA) and provided as a kit by ImmunoVision Technologies
11
12 (Daly City, CA) and consisted of a blocking solution (that also could be used as the
13
14 primary antibody diluent), a poly-HRP-labeled linker antibody (goat anti-mouse or
15
16 goat anti-rabbit IgG), and a chromogen substrate solution. CAP, streptomycin,
17
18 tetracycline and oxytetracycline and 6-mercaptohexanol (MCH) were purchased from
19
20 Sigma (Milan, Italy). Ferric chloride (FeCl₃·6H₂O), sodium acetate anhydrous (NaAc)
21
22 were purchased from Sinopharm Chemical Reagent Co., Ltd. (Beijing, China).
23
24 Hydrogen tetrachloroaurate (III) tetrahydrate (HAuCl₄), hydrogen peroxide (H₂O₂,
25
26 30%) were purchased from Sinopharm Chemical Reagent Co., Ltd. (Shanghai, China)
27
28 and 3, 3', 5, 5'-tetramethylbenzidine (TMB) and Poly diallyldimethylammonium
29
30 chloride solution (PDDA) were purchased from Sigma (USA). PBS buffer (pH 7.4,
31
32 0.1 M KH₂PO₄-K₂HPO₄, 0.1 M KCl) was used as washing and binding buffer. All
33
34 other reagents were all of analytical grade and were used without further purification.
35
36 Distilled water was used throughout the study.
37
38
39
40
41
42
43
44
45

46 2.2 Apparatus

47
48 The transmission electron microscopic (TEM) image was obtained with a H600
49
50 transmission electron microscope (Hitachi, Japan). Scanning electron micrographs
51
52 (SEM) images were obtained with a S3400N scanning electron microscope (Hitachi,
53
54 Japan). The UV-vis spectra were recorded on a UV-1800 spectrophotometer
55
56
57
58
59
60

(Shimadzu Co., Japan).

2.3 Preparation of AuNPs

AuNPs were prepared according to the Frens method with slight modifications.³⁴ Typically, 0.01 wt% HAuCl₄ (100 mL) was boiled and vigorously stirred in a flask. 1 wt% trisodium citrate solution (2.5 mL) was quickly added into this boiling solution and the color changed from grey, blue, purple, to wine red, which indicated the formation of AuNPs. The solution was maintained for another 10 minutes at boiling temperature, then cooled to room temperature and stored at 4 °C for further experiments.

2.4 Preparation of Fe₃O₄@Au nanospheres

Firstly, Fe₃O₄ nanospheres (Fe₃O₄ NPs) were prepared through a solvothermal reaction by Li's method.³⁵ In a typical procedure, 8.1 g FeCl₃·6H₂O and 21.6 g NaAc were dissolved in 300 mL ethylene glycol and stirring for 30 min to form a clear solution. Then the mixture solution was transferred to Teflon-lined stainless-steel autoclaves and hermetically heated at 200 °C. After reaction for 8 h, the autoclaves were cooled to room temperature. The obtained black products were collected by a magnet and washed several times with deionized water and ethanol respectively, then dried under vacuum at 60 °C for further use.

Fe₃O₄@Au nanospheres (AuMNPs) were synthesized according to the previously reported literature with minor modifications.³⁶ In brief, 0.02 g Fe₃O₄ NPs was dispersed in 5 mL 3% PDDA aqueous solution and then stirred for 30 min. After magnetic separation and removal of the unbounded PDDA, the resulting solid was

1
2
3
4 spreaded in 130 mL gold gum solution and stirred for 8 h at room temperature. The
5
6 dark purple AuMNPs were obtained until the supernatant was colorless through
7
8 magnetic separation. After washed several times with deionized water and ethanol
9
10 respectively, the AuMNPs were dispersed into 100 mL ultrapure water. Prior to use,
11
12 the solution was stored at 4 °C.
13
14

15 16 2.5 Preparation of the AuMNPs-Apt 17

18
19 The immobilization of aptamer onto AuMNPs was carried out according to the
20
21 previously reported with some modification.³⁷ First, 50 µL AuMNPs were washed for
22
23 several times with PBS buffer (pH 7.4), and then resuspended in 500 µL PBS buffer,
24
25 subsequently, ultrasonicated for 30 min. In order to fully integrate aptamers and
26
27 AuMNPs, excess of thiolated Apt (50 µM) was added into the above solution and
28
29 gently stirred for 12 h at room temperature. The superfluous Apt were removed
30
31 through magnetic separation. Next, the as-prepared AuMNPs-Apt was washed three
32
33 times with 500 µL PBS buffer. 500 µL, 1 mM MCH was then added and incubated for
34
35 about 30 min at room temperature to block the possible residual sites. The resulting
36
37 conjugates were finally re-suspended in 500 µL PBS buffer followed by washing and
38
39 magnetic separation. The final concentration of as-prepared capture probe was 38 mg
40
41 mL⁻¹ and then stored at 4 °C for further use. The remaining ratio of the magnetic bead
42
43 was obtained from the concentration ratio of as-prepared capture probe and Fe₃O₄ NPs.
44
45 And we can know that 0.02 g Fe₃O₄ NPs was finally resuspended in 500 µL PBS
46
47 buffer, the concentration of Fe₃O₄ NPs was 40 mg mL⁻¹. Thus, we could calculate the
48
49 remaining ratio of the magnetic bead after washing was 95%.
50
51
52
53
54
55
56
57
58
59
60

2.6 Preparation of the cDNA-AuNPs-PV conjugates

AuNPs co-immobilized with PV and cDNA were prepared according to the literature with some modification.³⁸ Briefly, 500 μL , 10 mg mL^{-1} AuNPs was initially adjusted to pH 9.0 by 0.1 M K_2CO_3 aqueous solution. Then, 20 μL PV reagents (the original concentration of PV in Kits) was added to the solution and incubated for 15 min at room temperature. In this process, PV was covalently bound to AuNPs through the dative binding between AuNPs and free -SH groups of the antibody on PV.³⁹ Afterward, 10 μL , 50 μM thiol-modified cDNA was injected into the mixture solution. Subsequently, the solution was kept for 24 h at 4 $^\circ\text{C}$, followed by centrifugation for 15 min at 10000 rpm. After the supernatant was discarded, the red pellets were washed several times with PBS buffer. Following that, 500 μL , 1 mM MCH was added and then incubated for about 30 min at room temperature to block the possible residual sites. The resulting cDNA-AuNPs-PV conjugates were finally resuspended in PBS buffer and stored at 4 $^\circ\text{C}$ for further use.

2.7 Preparation of colorimetric aptasensor for CAP detection

The fabrication procedures of the colorimetric aptasensor for CAP were illustrated in Scheme 1. Briefly, 40 μL , 38 mg mL^{-1} of as-prepared capture probe was added to excess amount of signal tag. The mixture solution was gently stirred for 45 min at 37 $^\circ\text{C}$ to obtain the hybridized biocomplex. And then the hybridization solution was collected by the external magnet. For determination of CAP, the above solution was incubated with 100 μL PBS containing different concentrations of CAP for 30 min at room temperature. Then cDNA-AuNPs-PV signal tags released from the

1
2
3
4 biocomplex were separated into the soluble supernatant with magnetic separation.
5
6 Subsequently, 50 μL , 0.2 mg mL^{-1} TMB and 0.015% H_2O_2 were added. Finally, the
7
8 mixture solution was shaken thoroughly for color development and the absorbance
9
10 was measured at 652 nm by UV-vis spectrometer for quantitative analysis. For
11
12 practical convenience, all measurements were conducted at room temperature.
13
14

15 16 2.8 Sample preparation

17
18 Fish and pork samples were purchased from retail supermarket in Ningbo, China.
19
20 These samples were triturated in a blender, freeze-dried, and stored at $-18\text{ }^\circ\text{C}$ before
21
22 analysis. All experiments were performed in compliance with the relevant laws and
23
24 institutional guidelines of Ministry of Agriculture of China. Moreover, fish and pork
25
26 collection and transportation activities were authorized by of Ministry of Agriculture
27
28 of China, license number CARS-43-17. Procedures involving animal handling and
29
30 experiment were approved by the Center of Experimental Animals (SCXK (HU)
31
32 2012-0002), Ningbo University, China.
33
34
35
36
37

38 3 Results and discussion

39 40 3.1 Construction and characterization of cDNA-AuNPs-PV conjugates

41
42 AuNPs, AuNPs-cDNA, cDNA-AuNPs-PV were characterized by TEM and
43
44 UV-vis spectrophotometry. The results were shown in Fig. 1. The size of AuNPs was
45
46 about 20 nm in diameter (Fig. 1A). Compared to bare AuNPs, some pearl chain-like
47
48 nanostructures were observed in AuNPs-cDNA composites (Fig. 1B). These results
49
50 indicated that the cDNA may be successfully assembled on the surface of AuNPs and
51
52
53
54
55
56 it can recognize aptamer on capture probe through the hybridization of
57
58
59
60

1
2
3
4 complementary sequences. After conjugating with PV on the AuNPs-cDNA, a shadow
5
6 and aggregated coating was observed around the dark AuNPs core (Fig. 1C). It meant
7
8 that PV was successfully modified on AuNPs-cDNA to form cDNA-AuNPs-PV
9
10 conjugates. Fig. 1D showed the UV-vis absorption spectrum of AuNPs, AuNPs-cDNA
11
12 and cDNA-AuNPs-PV conjugates. The bare AuNPs exhibited a characteristic
13
14 absorption peak at 520 nm (curve a), which was related to the surface plasmon
15
16 resonance of AuNPs. In curve b, a new absorption peak at 260 nm was observed,
17
18 which could be ascribed to the characteristic absorption peak of DNA. And the
19
20 characteristic absorption peak of AuNPs-cDNA showed a slight red shift from 520 to
21
22 522 nm compared with bare AuNPs. It meant that cDNA was successfully modified
23
24 on AuNPs. Moreover, as shown in curve c, a new absorption peak occurred at 385 nm
25
26 belongs to HRPs on PV was observed which meant the successful formation of
27
28 cDNA-AuNPs-PV conjugates.
29
30
31
32
33
34
35

36 Fig. 1

37 3.2 Characterization of AuMNPs-Apt

38
39
40
41 Fe_3O_4 NPs, AuMNPs samples were characterized by SEM and UV-vis
42
43 spectrophotometry. Fig. 2A depicted the average diameter of spherical Fe_3O_4 NPs was
44
45 about 350 nm with a rough surface. Fig. 2B was the SEM image of the AuMNPs and
46
47 showed many 20 nm AuNPs were adhered to the surface of the Fe_3O_4 NPs. In addition,
48
49 the ultraviolet visible absorption spectra of AuNPs (curve a), AuMNPs (curve b),
50
51 AuMNPs-Apt (curve c), Fe_3O_4 NPs (curve d) were shown in Figure 2C, respectively.
52
53
54
55
56
57
58
59
60 As shown in Fig. 2C, bare Fe_3O_4 NPs has no absorption peak from 300 to 800 nm.

1
2
3
4 However, AuMNPs had a maximum absorption peak at 522 nm and showed a slight
5
6 red shift from 520 to 522 nm. The phenomenon may be attributed to the interaction
7
8 between AuNPs and Fe₃O₄ NPs. Hence, we could conclude that AuNPs maybe
9
10 successfully assembled on Fe₃O₄ NPs surface. A new absorption peak at 262 nm was
11
12 also observed on the UV-vis absorption spectrum of AuMNPs-Apt, which indicating
13
14 that the aptamer was successfully bound onto AuMNPs.
15
16
17

18
19 To further verify the successful preparation of AuMNPs-Apt, the following
20
21 experiment was proposed. The conjugation of AuMNPs with aptamers was
22
23 characterized by UV-vis absorption spectrum, as shown in Fig. 2D. Before
24
25 conjugation to AuMNPs, the strong absorbance of aptamers can be seen at about 260
26
27 nm (curve a). After incubation of AuMNPs and aptamers, the supernatant was
28
29 gathered with magnetic separation. The absorbance of the supernatant was much
30
31 weaker at 260 nm (curve b), which was due to part of the aptamers successfully
32
33 combined with AuMNPs. Vibrating sample magnetometry (VSM) was employed to
34
35 evaluate the magnetic properties of Fe₃O₄ NPs, AuMNPs and AuMNPs-Apt. Details
36
37 have been presented in Section S1.1 of Supplementary material.
38
39
40
41
42
43
44

45
46
47
48
49
50
51
52
53
54
55
56
57
58
59
60
Fig. 2

3.3 Principle of colorimetric aptasensor for CAP detection

In order to verify this detection principle, some controlled experiments were performed. Fig. 3 showed the UV-vis spectrum of TMB solution under various conditions. It can be seen that, in the absence (curve a) and in the presence (curve b) of H₂O₂, TMB solution exhibited no characteristic peak in the range of 500 - 800

1
2
3
4 nm.⁴⁰ Moreover, in the presence of AuNPs-cDNA, the TMB-H₂O₂ mixture solution
5
6 also exhibited no characteristic peak. However, the TMB-H₂O₂ mixture solution
7
8 exhibited a strong absorption peak at 652 nm after the cDNA-AuNPs-PV conjugates
9
10 was added for about 5 min at room temperature, which should be attributed to the
11
12 redox reaction of TMB-H₂O₂ caused by HRPs on PV. The inset in Fig. 3 showed the
13
14 corresponding photo images. It was showed that the color of TMB solution (curve a),
15
16 TMB-H₂O₂ solution (curve b) and TMB-H₂O₂/AuNPs-cDNA solution (curve c) were
17
18 not changed. However, after 80 μ L cDNA-AuNPs-PV conjugates were added into
19
20 TMB-H₂O₂ solution, a dramatic color change and a strong absorption peak at 652 nm
21
22 were observed in curve d. Consequently, it can be inferred from the above
23
24 phenomenon that PV can greatly catalyze the redox reaction of TMB with H₂O₂.
25
26
27
28
29
30

31
32 Fig. 3

33 34 3.4 Comparison of colorimetric aptasensor responses using various labels

35
36 In order to acquire a high sensitivity of the aptasensor, it is extremely critical to
37
38 amplify the colorimetric responses by choosing favorable signal tags. Hence, we
39
40 performed four controlled experiments by adding AuNPs-cDNA, PV-cDNA,
41
42 cDNA-AuNPs-HRP and cDNA-AuNPs-PV signal tags into the TMB-H₂O₂ solution at
43
44 the same concentration (10 mg mL⁻¹), respectively. As shown in Fig. 4a, the TMB
45
46 solution exhibited no absorption peak from 500 to 800 nm due to the slow oxidizing
47
48 ability of H₂O₂ without peroxidase. And in the presence of AuNPs-cDNA, the
49
50 TMB-H₂O₂ mixture solution also exhibited no characteristic peak (Fig. 4b). However,
51
52 Fig. 4c exhibited an obvious absorption peak at 652 nm with the addition of
53
54
55
56
57
58
59
60

1
2
3
4
5
6
7
8
9
10
11
12
13
14
15
16
17
18
19
20
21
22
23
24
25
26
27
28
29
30
31
32
33
34
35
36
37
38
39
40
41
42
43
44
45
46
47
48
49
50
51
52
53
54
55
56
57
58
59
60

PV-cDNA. From Fig. 4b and 4c, we could conclude that the absorption peak was ascribed to the oxidative product of TMB by H₂O₂ in the presence of HRP enzymes on PV instead of AuNPs. Additionally, compared with PV-cDNA (Fig. 4c), cDNA-AuNPs-PV (Fig. 4e) displayed a higher absorption peak, which showed that AuNPs have the ability to gather more PVs on signal tags and then strengthen the catalytic ability. In Fig. 4e, a significantly increased absorption peak (about 15-fold higher than Fig.4d) can be observed at 652 nm while adding cDNA-AuNPs-PV into the TMB-H₂O₂ solution. This phenomenon showed that cDNA-AuNPs-PV has higher catalytic response towards TMB with H₂O₂ than cDNA-AuNPs-HRP, which should be attributed to much more HRPs on AuNPs-PV than AuNPs-HRP. It can be concluded that PV has an excellent signal amplification effect to achieve high sensitivity for the colorimetric aptasensor.

Fig. 4

3.5 Optimization of experimental conditions

To obtain an optimal analytical performance, various conditions, such as the concentration of TMB and H₂O₂, the volume of PV and the incubation time, were optimized in this study including the pH of detection solution.

The pH value of the detection solution played an important role in the response of the colorimetric aptasensor. Fig. S2 (A) illustrated the effect of pH from 5.0 to 9.0 on the absorbance response. With the increasing solution pH, the absorbance intensity increased and achieved a maximum value at pH 7.0. Herein we chose pH 7.0 PBS solution as the optimal buffer.

1
2
3
4 Fig. S2 (B) exhibited the absorbance of various concentrations of TMB. With the
5
6 increasing concentration of TMB, the absorbance sharply increased and reached to a
7
8 steady value when a higher concentration of TMB ($> 0.2 \text{ mg mL}^{-1}$) was used.
9
10 Therefore, 0.2 mg mL^{-1} was chosen as the favorable TMB concentration. In addition,
11
12 the concentration of H_2O_2 was also investigated. As shown in Fig. S2 (C), the
13
14 absorbance intensity increased rapidly with the increasing concentration of H_2O_2 .
15
16 However, no further increase of the absorbance was observed when the H_2O_2
17
18 concentration was over 0.015%. Thus, 0.015% was selected as the favorable
19
20 concentration to receive high signal response.
21
22
23
24

25
26 For sensitivity study, the effect of the volume of PV was also optimized. Fig. S2
27
28 (D) showed the absorbance value from $5 \mu\text{L}$ to $30 \mu\text{L}$ of PV (the original
29
30 concentration of PV in Kits) in the AuNPs-cDNA composite solution to prepare the
31
32 signal tag, and the largest absorbance value was obtained at $20 \mu\text{L}$ of PV. In this test,
33
34 $20 \mu\text{L}$ of PV was chosen as the optimal volume. Fig. S2 (E) showed the signal
35
36 response between AuMNP-Apt/cDNA-AuNPs-PV hybridization composites and
37
38 CAP target in the range from 10 min to 60 min. At first, the absorption peak at 652 nm
39
40 increased with the increasing incubation time. However, the signal response reached
41
42 to a plateau when the reaction time was higher than 30 min. This phenomenon
43
44 indicated that the reaction of aptamer with CAP reached to equilibrium. Thus, 30 min
45
46 could be chosen for the favorable incubation time. In addition, the response time of
47
48 the detection for measurement sample from 1 min to 20 min was also examined, as
49
50 shown in Fig. S2 (F). The results showed that the absorbance intensity first increased
51
52
53
54
55
56
57
58
59
60

1
2
3
4 and then stabilized after 10 min. This indicated that 10 min was selected as the
5
6 favorable response time.
7

8 9 3.6 Analytical performance of the colorimetric aptasensor

10
11 Under the optimal detection conditions, the catalytic ability of PV on TMB
12 oxidation was investigated. The colorimetric aptasensor was used for quantitatively
13 detecting different concentrations of target CAP based on the absorbance at 652 nm
14 (Fig. 5). Obviously, the absorbance density increased gradually with increasing
15 concentration of target CAP (Fig. 5A). The standard calibration curve of the ΔA (ΔA
16 $=A-A_0$, where A_0 and A are the absorbance at 652 nm in the absence and presence of
17 CAP, respectively) for CAP detection in the range from 0.05 to 200 ng mL⁻¹ was
18 shown in Fig. 5B. The detection limit (LOD) was 0.02 ng mL⁻¹. Moreover, the color
19 changes of different concentrations of target CAP were recorded by digital camera. As
20 shown in Fig. 5C, an obvious change from colorless to light blue could be
21 distinguished with naked eyes when the concentration of CAP is over 0.1 ng mL⁻¹.
22 The analytical properties are comparable or even better than previous reports on CAP
23 detection shown in Table S1. These advantages of the assay may lead to the
24 significant change of the absorbance and greatly improve the sensitivity.
25
26
27
28
29
30
31
32
33
34
35
36
37
38
39
40
41
42
43
44
45

46 Fig. 5

47 48 49 3.7 Specificity, reproducibility and stability of the proposed aptasensor

50
51 To further evaluate the specificity and selectivity of the developed colorimetric
52 aptasensor, we challenged the assay with several possible components in real samples,
53 such as streptomycin (STR), tetracycline (TC) and oxytetracycline (OTC). They were
54
55
56
57
58
59
60

1
2
3
4 added into the incubation solution with the same concentration of 1000 ng mL⁻¹,
5
6 respectively. The assay was implemented by the above developed method. As
7
8 indicated in Fig. 6, higher absorbance values were observed with target CAP (5 ng
9
10 mL⁻¹) toward 200-fold higher interfering substances. The absorbance in the presence
11
12 of STR, TC and OTC was almost the same as the control sample. More significantly,
13
14 the absorbance of the mixture containing target CAP and interfering substances was
15
16 not significantly changed compared with target CAP alone. Therefore, the results
17
18 revealed that the developed colorimetric aptasensor was sufficiently selective for the
19
20 target CAP.
21
22
23
24

25
26 The reproducibility of the proposed colorimetric aptasensor was evaluated
27
28 according to intra-assay and inter-assay precision. We evaluated the intra-assay
29
30 precision by assaying a standard sample for six repeated measurements. The
31
32 inter-assay precision was evaluated by assaying a standard sample in six assays
33
34 performed identically. The coefficient of variation (CV) of intra-assay was 4.5% for
35
36 50 ng mL⁻¹ CAP and the inter-assay was 7.9% for 50 ng mL⁻¹ CAP. Additionally, the
37
38 stability was also investigated. After the AuMNPs-Apt and cDNA-AuNPs-PV were
39
40 stored at 4 °C for 29 days, they still remained 93.2% and 94.6% of the initial
41
42 responses of colorimetric, indicating that the proposed aptasensor possess good
43
44 stability.
45
46
47
48
49
50

51
52 Fig. 6

53 54 3.8 Application in real samples

55
56 In order to validate the feasibility and application potential of the proposed
57
58
59
60

1
2
3
4 colorimetric aptasensor, the detection of CAP in fish and pork samples was assayed,
5
6 respectively. The real samples were spiked with various concentrations of CAP. The
7
8 results analyzed using the proposed method were compared with the reference values
9
10 obtained using the commercially ELISA method. The results were shown in Table 1.
11
12 The recoveries of the CAP standards in fish sample are 99.9% to 102%, while 98% to
13
14 100.5% in pork sample. These desirable recoveries definitely indicated the reliability
15
16 of the proposed method for detection of CAP in fish and pork samples.
17
18
19
20

21 Table 1
22

23 24 **4 Conclusion**

25
26 This work demonstrated a novel and sensitive colorimetric aptasensor for CAP
27
28 determination based on cDNA-AuNPs-PV conjugates for signal amplification. The
29
30 carried PV labeled on signal tags could greatly catalyze the H₂O₂-mediated oxidation
31
32 of TMB, causing a dramatic color change and resulting in the change of the UV-vis
33
34 absorbance. The absorbance at 652 nm linearly increased with the increment of CAP
35
36 concentration. The absorbance at 652 nm linearly increased with the increment of CAP
37
38 concentration. The method detection limit down to 0.02 ng mL⁻¹ was measured by
39
40 UV-vis absorption spectroscopy and 0.1 ng mL⁻¹ of CAP can be clearly distinguished
41
42 with naked eyes. More importantly, this proposed method had been successfully
43
44 applied in fish and pork samples. Compared with the conventional methods, the
45
46 designed assay is cheaper, faster and more specific, and offers great potential for
47
48 application in on-site detection by controlling aptamer.
49
50
51
52
53
54

55 56 **Acknowledgements** 57 58 59 60

1
2
3
4 This work is financially supported by the Projects of Zhejiang Public Benefit
5
6 Research Project of China (2014C32051), Science & Technology of Ministry of P.R.
7
8 China (2012BAK08B01-2 & 2013GB2C200191), East China Sea Mariculture
9
10 Collaborative Innovation Center, National Waterfowl Industry System (CARS-43-17)
11
12 and the Natural Science Foundation of Zhejiang and Ningbo (Y15B050008,
13
14 2013A610163, 2014A610184), The KC Wong Magna Fund in Ningbo University.
15
16
17
18
19
20
21
22
23
24
25
26
27
28
29
30
31
32
33
34
35
36
37
38
39
40
41
42
43
44
45
46
47
48
49
50
51
52
53
54
55
56
57
58
59
60

References

- 1 A. Wang, L. Zhang, Y. Fang, *Anal. Chim. Acta*, 394, 1999, 309-316.
- 2 X. Que, D. Tang, B. Xia, M. Lu, D. Tang, *Anal. Chim. Acta*, 830, 2014, 42-48.
- 3 L. Wang, Y. Zhang, X. Gao, Z. Duan, S. Wang, *J. Agric. Food. Chem.*, 58, 2010, 3265-3270.
- 4 H. Wang, X. Zhou, Y. Liu, H. Yang, Q. Guo, *J. Agric. Food. Chem.*, 59, 2011, 3532-3538.
- 5 M. Ramos, P. Munoz, A. Aranda, I. Rodriguez, R. Diaz, J. Blanca, *J. Chromatogr. B*, 791, 2003, 31-38.
- 6 M. Yuan, W. Sheng, Y. Zhang, J. Wang, Y. Yang, S. Zhang, I. Goryacheva and S. Wang, *Anal. Chim. Acta*, 751, 2012, 128-134.
- 7 B. Berendsen, M. Pikkemaat, P. Römken, R. Wegh, M. van Sisseren, L. Stolker, M. Nielen, *J. Agric. Food. Chem.*, 61, 2013, 4004-4010.
- 8 J. Xu, W. Yin, Y. Zhang, J. Yi, M. Meng, Y. Wang, H. Xue, T. Zhang, R. Xi, *Food Chem.*, 134, 2012, 2526-2531.
- 9 X. Yu, Y. He, J. Jiang, H. Cui, *Anal. Chim. Acta*, 812, 236-242.
- 10 C. Douny, J. Widart, E. De Pauw, G. Maghuin-Rogister, M. Scippo, *Food Anal. Method.*, 6, 2013, 1458-1465.
- 11 Q. Zhang, T. Peng, D. Chen, J. Xie, X. Wang, G. Wang, C. Nie, *J. AOAC Int.*, 96, 2013, 897-901.
- 12 J. Han, Y. Wang, C. Yu, Y. Yan, X. Xie, *Anal. Bioanal. Chem.*, 399, 2011, 1295-1304.

- 1
2
3
4 13 T. Sniegocki, A. Posyniak, M. Gbylik-Sikorska, J. Zmudzki, *Anal. Lett.*, 47, 2014,
5
6 568-578.
7
8
9 14 N. Liu, S. Song, L. Lu, D. Nie, Z. Han, X. Yang, Z. Zhao, A. Wu, X. Zheng, *Food*
10
11 *Agr. Immunol.*, 25, 2014, 523-534.
12
13 15 T. Alizadeh, M. Ganjali, M. Zare, P. Norouzi, *Food Chem.*, 130, 2012, 1108-1114.
14
15 16 S. Yadav, B. Agrawal, P. Chandra, R. Goyal, *Biosens. Bioelectron.*, 55, 2014,
16
17 337-342.
18
19 20
21 21 A. Ellington, J. Szostak, *Nature*, 346, 1990, 818-822.
22
23 24 S. Pilehvar, T. Dierckx, R. Blust, T. Breugelmans, K. De Wael, *Sensors*, 14, 2014,
24
25 12059-12069
26
27 28
29 29 M. Zhao, Y. Zhuo, Y. Chai, Y. Xiang, N. Liao, G. Gui, R. Yuan, *Analyst*, 138, 2013,
30
31 6639-6644.
32
33 34 Z. Lv, A. Chen, J. Liu, Z. Guan, Y. Zhou, S. Xu, C. Li, *PloS one*, 9, 2014, e85968.
34
35 36 A. Keefe, S. Pai, A. Ellington, *Nat. Rev. Drug. Discov.*, 9, 2010, 537-550.
36
37 38
39 39 Y. Kim, J. Jurng, *Sens. Actuators, B: Chem.*, 176, 2013, 253-257.
40
41 42 R. Luo, Y. Li, X. Lin, F. Dong, W. Zhang, L. Yan, W. Cheng, H. Ju, S. Ding, *Sens.*
42
43 *Actuators, B: Chem.*, 198, 2014, 87-93.
44
45 46 X. Xiang, L. Chen, Q. Zhuang, X. Ji, Z. He, *Biosens. Bioelectron.*, 32, 2012,
46
47 43-49.
48
49 50
51 52 L. Ou, P. Jin, X. Chu, J. Jiang, R. Yu, *Anal. Chem.*, 82, 2010, 6015-6024.
52
53 54 H. Liu, Y. Wang, J. Wang, J. Xue, B. Zhou, H. Zhao, S. Liu, X. Tang, S. Chen, M.
54
55 Li, J. Cao, *Anal. Biochem.*, 458, 2014, 4-10.
56
57
58
59
60

- 1
2
3
4 27 Y. Yin, Y. Cao, Y. Xu, G. Li, *Int. J. Mol. Sci.*, 11, 2010, 5077-5094
5
6 28 S. Shi, J. Guo, R. Cote, L. Young, D. Hawes, Y. Shi, S. Thu, C. Taylor, *Appl.*
7
8 *Immunohistochem. Mol. Morphol.*, 7, 1999, 201-208.
9
10 29 T. Yu, W. Cheng, Q. Li, C. Luo, L. Yan, D. Zhang, Y. Yin, S. Ding, *Talanta*, 93,
11
12 2012, 433-438.
13
14 30 Z. Zhou, W. Wei, Y. Zhang, S. Liu, *J. Mater. Chem. B*, 22, 2013, 2851-2858.
15
16 31 K. Lee, V. Scardaci, H. Kim, T. Hallam, H. Nolan, B. Bolf, G. Maltbie, J. Abbott, G.
17
18 *Duesberg, Sens. Actuators B: Chem.*, 188, 2013, 571-575.
19
20 32 J. Mehta, B. Van Dorst, E. Rouah-Martin, W. Herrebout, M. Scippo, R. Blust, J.
21
22 *Robbens, J. Biotechnol.*, 155, 2011, 361-369
23
24 33 L. Yan, C. Luo, W. Cheng, W. Mao, D. Zhang, S. Ding, *J. Electroanal. Chem.*, 687,
25
26 2012, 89-94.
27
28 34 G. Frens, *Nature*, 241, 1973, 20-22.
29
30 35 H. Dong, X. Li, Q. Peng, X. Wang, J. Chen, Y. Li, *Angew. Chem. Int. Ed.*, 44, 2005,
31
32 2782-2785.
33
34 36 X. Chen, J. Zhu, Z. Chen, C. Xu, Y. Wang, C. Yao, *Sens. Actuators B: Chem.*, 159,
35
36 2011, 220-228.
37
38 37 J. Zhao, Y. Zhang, H. Li, Y. Wen, X. Fan, F. Lin, L. Tan, S. Yao, *Biosens.*
39
40 *Bioelectron.*, 26, 2011, 2297-2303.
41
42 38 B. Zhang, B. Liu, D. Tang, R. Niessner, G. Chen, D. Knopp, *Anal. Chem.*, 84, 2012,
43
44 5392-5399.
45
46 39 G. Hermanson, *Bioconjugate Techniques*, 2nd ed.; San Diego: Academic Press,
47
48
49
50
51
52
53
54
55
56
57
58
59
60

1
2
3
4 2008, 1202.
5

6 40 Y. Song, K. Qu, C. Zhao, J. Ren, X. Qu, Adv. Mater., 22, 2010, 2206-2210.
7
8
9
10
11
12
13
14
15
16
17
18
19
20
21
22
23
24
25
26
27
28
29
30
31
32
33
34
35
36
37
38
39
40
41
42
43
44
45
46
47
48
49
50
51
52
53
54
55
56
57
58
59
60

Table 1

Recoveries of CAP comparison of two methods obtained in the spiked fish and pork samples (n = 3).

Sample type	CAP Added (ng mL ⁻¹)	The proposed method	Conventional ELISA	Recovery of the method (%)
		CAP Detected (ng mL ⁻¹)	CAP Detected (ng mL ⁻¹)	
Fish	blank	0.28 ± 0.04	0.21 ± 0.05	/
	0.5	0.79 ± 0.12	0.68 ± 0.06	102.0
	20	20.48 ± 0.33	20.32 ± 0.18	101.0
	50	50.23 ± 0.24	50.13 ± 0.31	99.9
Pork	blank	0.08 ± 0.01	-	/
	0.5	0.57 ± 0.04	0.49 ± 0.04	98.0
	20	20.18 ± 0.34	19.84 ± 0.13	100.5
	50	49.58 ± 0.56	48.75 ± 0.35	99.0

a The symbol '-' suggest that the sample could not be detected by the corresponding method.

Figure captions:

Scheme 1. Scheme of depicting the proposed colorimetric aptasensor to detect CAP using cDNA-AuNPs-PV as signal tags.

Fig. 1. TEM images of (A) bare AuNPs, (B) AuNPs-cDNA conjugates, (C) cDNA-AuNPs-PV conjugates, (D) UV-vis spectra of AuNPs (a), AuNPs-cDNA conjugates (b) and cDNA-AuNPs-PV conjugates (c).

Fig. 2. SEM images of (A) Fe₃O₄ NPs, (B) AuMNPs, (C) UV-vis spectra of AuNPs (a), AuMNPs (b), AuMNPs-Apt (c) and Fe₃O₄ NPs (d), (D) UV-vis spectra of initial aptamer solution (a), supernatant liquor after aptamer conjugation to AuMNPs (b).

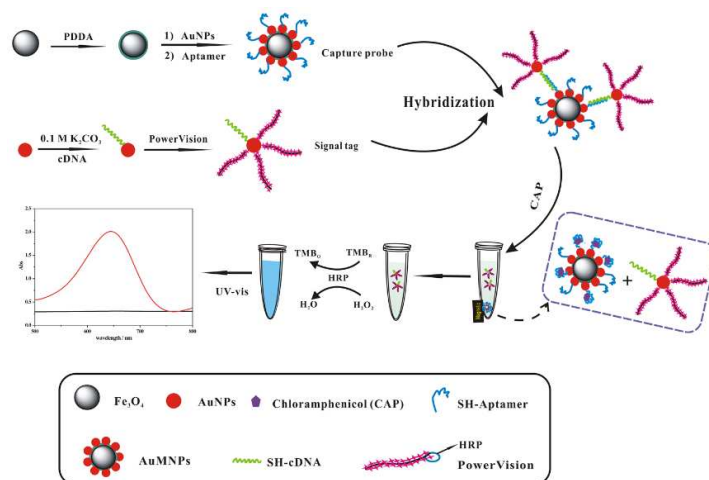
Fig. 3. UV-vis spectra of TMB solution in the absence (black) and presence (red) of H₂O₂, TMB-H₂O₂ solution catalyzed by AuNPs-cDNA (blue), and TMB-H₂O₂ solution catalyzed by cDNA-AuNPs-PV (pink) as signal tag. Inset shows the corresponding digital camera pictures of TMB solution (a), TMB-H₂O₂ solution (b), TMB-H₂O₂/ AuNPs-cDNA (c) and TMB-H₂O₂/cDNA-AuNPs-PV (d), respectively.

Fig. 4. UV-vis spectra of TMB solution after the reaction with H₂O₂ (a), TMB-H₂O₂ mixture solution catalyzed by using various labels AuNPs-cDNA (b), PV-cDNA (c), cDNA-AuNPs-HRP (d), cDNA-AuNPs-PV (e) at the same concentration (10 mg mL⁻¹), respectively.

Fig. 5. (A) UV-vis absorption spectra of the proposed colorimetric aptasensor in the presence of different concentrations of CAP target, (B) calibration plot of the proposed colorimetric aptasensor in the presence of different concentrations of CAP target, (C) Photographs of colorimetric responses of different amounts of target CAP.

1
2
3
4 From a to g: the concentration of CAP are 0, 0.05, 0.1, 5, 20, 50, 100 ng mL⁻¹,
5
6 respectively.
7

8
9 **Fig. 6.** The specificity of the developed colorimetric aptasensor.
10
11
12
13
14
15
16
17
18
19
20
21
22
23
24
25
26
27
28
29
30
31
32
33
34
35
36
37
38
39
40
41
42
43
44
45
46
47
48
49
50
51
52
53
54
55
56
57
58
59
60



Scheme 1

1
2
3
4
5
6
7
8
9
10
11
12
13
14
15
16
17
18
19
20
21
22
23
24
25
26
27
28
29
30
31
32
33
34
35
36
37
38
39
40
41
42
43
44
45
46
47
48
49
50
51
52
53
54
55
56
57
58
59
60

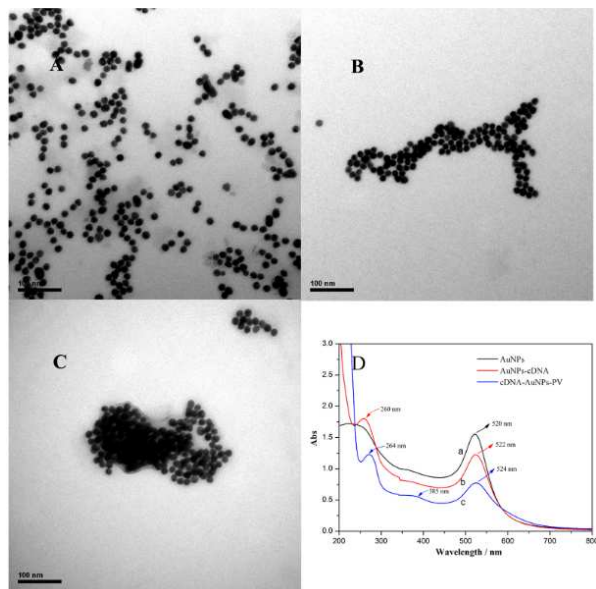


Fig. 1

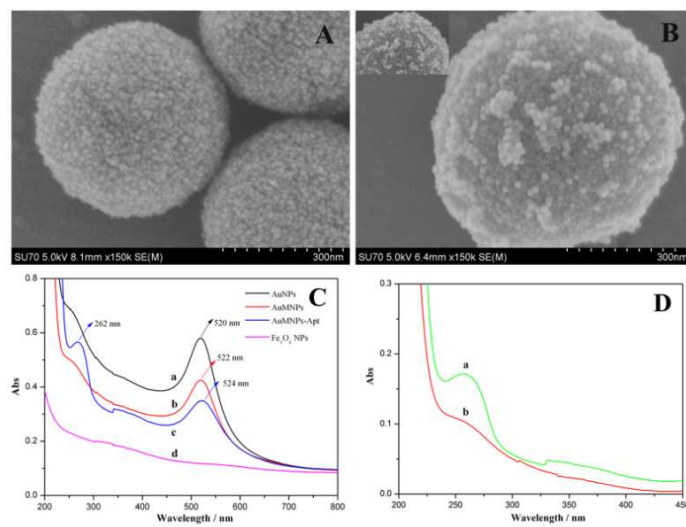


Fig. 2

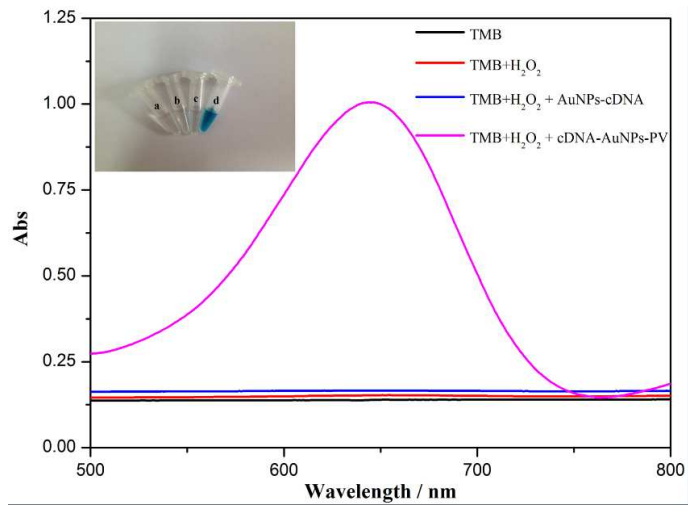


Fig. 3

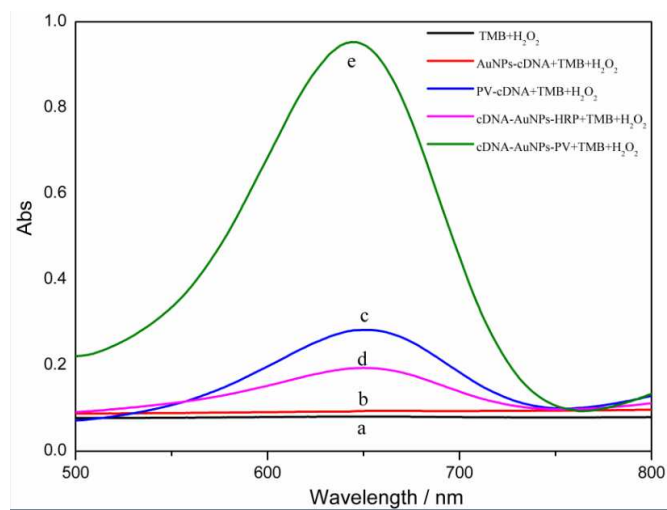


Fig. 4

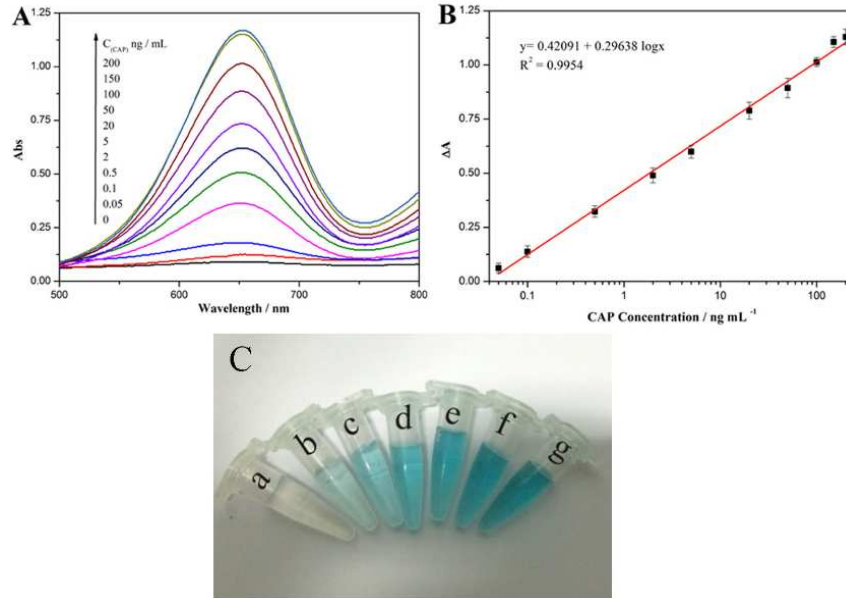


Fig. 5

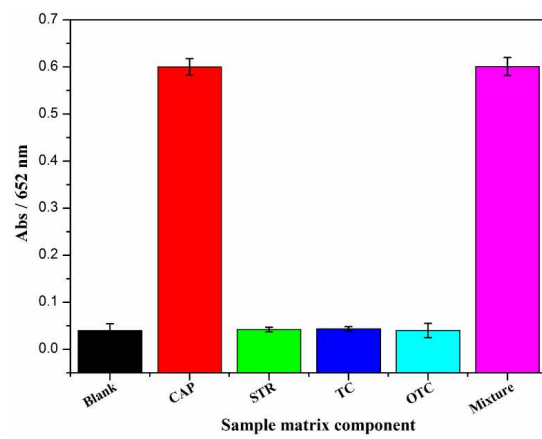
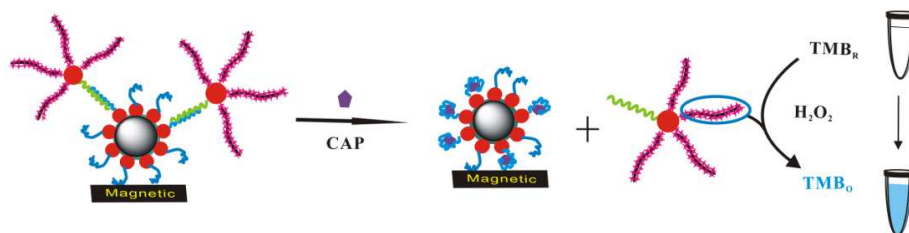


Fig. 6

Graphical abstract



The polymerase chain (PV), labeled gold colloid as signal tag, could greatly catalyze the H_2O_2 -mediated oxidation of TMB for color development, which can be easily observed with naked eyes and quantified by UV spectroscopy.